Available online at www.sciencedirect.com
SCIENCE DIRECT®
Polymer 44 (2003) 4435–4441
polymer
www.elsevier.com/locate/polymer

Epoxy-silica polymers as restoration materials. Part II

P. Cardiano[a,*], P. Mineo[b], S. Sergi[a], R.C. Ponterio[c], M. Triscari[d], P. Piraino[a]

[a]*Dipartimento di Chimica Inorganica, Chimica Analitica e Chimica Fisica, University of Messina, Salita Sperone 31 S. Agata, 98166 Messina, Italy*
[b]*CNR-Istituto di Chimica e Tecnologia dei Polimeri (sez. Catania), Viale A. Doria 6, 95125 Catania, Italy*
[c]*CNR-Istituto Processi Chimico-Fisici (sez. Messina), Via G. La Farina 237, 98123 Messina, Italy*
[d]*Dipartimento di Scienze della Terra, University of Messina, Salita Sperone 31-S. Agata, 98166 Messina, Italy*

Received 27 January 2003; received in revised form 28 April 2003; accepted 15 May 2003

Abstract

Room temperature reaction of the epoxy resin poly(bisphenolA-*co*-epichlorohydrin), glycidyl end-capped with the coupling agent (3-aminopropyl)triethoxysilane, in 1:2 (**1**), 1:1 (**2**) and 2:1 (**3**) molar ratios, leads, after curing for three months at room temperature, to glassy, transparent, crack-free solids which were investigated by SEM, TGA, DSC, NIR and Raman spectroscopy. SEM investigations show substantially a great homogeneity over the entire area with absence of cracks, veins and/or fissures and without formations of clusters and/or aggregates. The conversion of oxirane rings, as found by Raman spectroscopy, decreases by increasing the epoxy/amine ratio, with conversion percentages ranging from 95.3 to 81.3%. As a common feature, the presence in **1**, **2** and **3** of Si–O–Si linkages increases the polymer degradation temperature and thermal oxidative stability relative to the parent epoxy resin by shifting the weight loss to higher temperatures. Differently from mixtures **2** and **3**, which show the T_g at 90 °C, the mixture **1** does not exhibit any detectable glass transition.

Keywords: Hybrid materials; Epoxy polymers; Conservation

1. Introduction

A survey of the literature reports on the safeguard of architectural heritage clearly shows that a variety of epoxy resins are being used for the consolidation of stone monuments in an outdoor environment [1,2]. But these materials, besides to susceptibility to weathering and UV radiations, suffer, owing to their high molecular weight, from low penetration depth, which is a key factor of a preserving material. Large molecules may be confined in the surface region overstrengthening the superficial layer, which by the time undergoes detachment. Aimed to open new opportunities in the area of stone conservation materials, in the previous paper [3] we reported on the synthesis of epoxy-silica materials obtained by inducing polymerization on the epoxy monomer 3-glycidoxypropyl-trimethoxysilane through the primary amine (3-aminopropyl)triethoxysilane (ATS) in different molar ratios. The glassy materials, cured at room temperature for four months, are featured, as found by ^{29}Si CP-MAS NMR, by a high percentage of siloxane bonds and a condensation degree which ranges from 91 to 95%. Furthermore on the inorganic side, the polymer exhibits a predominating content of the tetrafunctional building group $RSi(OSi)_3$ while residual epoxy fragments are still present in the solid structure for lower amine content mixtures. The above materials offer the advantage that the polymerization can occur inside the stone starting from low-molecular weight monomers. This procedure allows rapid diffusion and penetration deep enough to exceed the maximum moisture zone as well as go beyond the damaged layer. Furthermore the hydrolytically unstable alkoxysilane groups easily generate silanole groups which, beside the self-condensation with consequent cross-linking, may covalently bind to OH fragments present in the stone anchoring the organic polymer to the lithic substrate.

As a continuation of the previous work we report here on the self-condensation of the epoxy resin poly(bisphenolA-*co*-epichlorohydrin), glycidyl end-capped (DGEBA) previously functionalized by using the coupling agent ATS (Fig. 1). The morphological details of the above materials as well as their NIR, Raman, TGA and DSC characterization are also presented. Epoxy polymers end-capped with

* Corresponding author. Tel.: +39-90-6765712; fax: +39-90-393756.
E-mail address: cardiano@chem.unime.it (P. Cardiano).

0032-3861/03/$ - see front matter © 2003 Elsevier Science Ltd. All rights reserved.
doi:10.1016/S0032-3861(03)00432-4

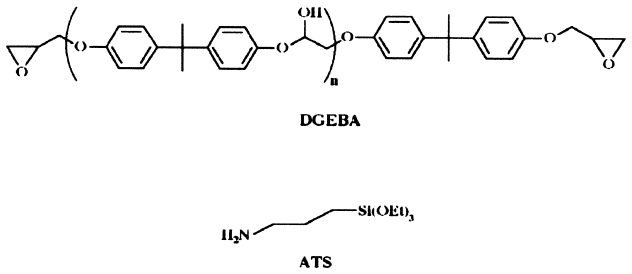

Fig. 1. DGEBA and ATS.

trialkoxysilane fragments have been frequently used to facilitate cross-linking between the polymer and growing inorganic network leading to organic–inorganic hybrid materials [4–8]. Virtually unexplored are the materials arising from self-condensation of the end-capped polymers.

2. Experimental section

Poly(bisphenolA-*co*-epichlorohydrin), glycidyl end-capped (Average $M_n = 348$ corresponding to an average degree of polymerization of 0.03; epoxy equivalent = 174) (DGEBA) was purchased from Aldrich Chemie, ATS (hydrogen equivalent = 110.6) from Fluka and used as received. ^{13}C NMR spectra were recorded on a Bruker AMX R-300 spectrometer operating at 75.47 MHz. FT-IR spectra were obtained on Perkin–Elmer RX-I on KBr disks. FT-NIR absorbance measurements were performed, using a Perkin–Elmer spectrometer, in the spectral range of 5000–4000 cm^{-1}. The used spectral resolution was of 4 cm^{-1} and 32 repetitive scans were automatically added to obtain a good signal-to-noise ratio and a spectra reproducibility of high quality. A U1000 ISA Raman spectrometer was used to collect the Raman spectra. The system is equipped with an optical microscope (BX-40 Olympus), which conveys the radiation of an Argon ion laser ($\lambda = 514.5$ nm), working at a power of 200 mW, to the sample. The Raman scattered beam, focalised in a spot of 0.5–1.0 μm diameter, was analysed employing a backscattering configuration through the microscope objective and collected by a CCD detector cooled with liquid N_2. The elastic Rayleigh line was filtered by holographic notch filters before reaching the detector. For all the samples a number of measurements, covering a spectral range of 1800–500 cm^{-1}, were performed in order to verify their similarity. A particular regard was used in the treatment of 1270–1200 cm^{-1} spectral data. Exact peak positions were determined using a fitting software package (PeakFit 4, AISN soft. Inc.) assuming a convoluted Gaussian–Lorentzian peaks profile. SEM + EDX investigations were carried out on a LEO S420 equipped with an Oxford LINK system ISIS 3000 working at an energy of 20 keV, an I probe of 50 pA and a working distance of 11 mm. All observations were performed from low to higher magnifications up to about 43000 X. Thermogravimetric analysis (TGA) was performed with a Perkin–Elmer TGA 7 analyzer equipped with a TAC 7/DX processor. All acquisition and data analysis was performed with Pyris Software (Ver. 2.04) by Perkin–Elmer Corporation. Investigations were performed in the temperature range between 50 and 800 °C with a heating rate of 10 °C/min under nitrogen or air atmosphere (50 mL/min). Differential scanning calorimetry (DSC) was performed using a Mettler DSC-20 furnace and a TC11 processor. The heating rate was 10 °C/min, under N_2 atmosphere. T_g measurements were performed on samples dried at 50 °C under vacuum to eliminate the volatiles trapped into the pore network which could hide other concomitant thermal processes.

3. Results and discussion

Epoxy cross-linking and inorganic cross-linking are concomitant processes which may occur when DGEBA and ATS are reacted since the latter may self-catalyze the hydrolysis and condensation of the $Si(OR)_3$ groups via nucleophilic attack of hydroxyl anions [9], as well as easily react with the oxirane ring with the formation of secondary or tertiary amines. Previous attempts to functionalize DGEBA by ATS failed since the experimental conditions (in bulk at 90 °C) produced rapid gelation [5].

When 1 g of DGEBA (3 mmol), dissolved in 10 ml of $CHCl_3$, was allowed to react in an open vessel, at room temperature, with ATS in1:2 (**1**), 1:1 (**2**) and 2:1 (**3**) molar ratios, an increase of the viscosity was observed until the formation, after 24 h, of rubbery solids. This suggests that air moisture is involved in the hydrolysis of the $Si(OR)_3$ groups. On the contrary, when the reaction is performed in a glass container sealed with parafilm the resulting mixtures remain liquid for 20 days. Slow evaporation of the volatiles through a few pinholes made on the top of the parafilm leads, in one week, to glassy solids, visually transparent and without polymerization shrinkage. The rate of the transition sol–gel–solid phase decreases and the gelation time appears dependent on the molar ratio, with the low ratio mixture featured by the longest gelation time. The course of the oxirane ring opening and the hydrolysis of the $Si(OR)_3$ groups have been followed in an NMR tube by j-mod pulse sequence ^{13}C NMR spectra until the liquid phase was present. As it concerns the organic part, the spectra of **1** experience the progressive disappearance of the resonances of the α carbon of ATS centered at 44.83 ppm as well as the band at 44.54 and 50.02 ppm due to the methylenic and CH carbons of the epoxy groups indicating the complete conversion of the reactive groups of ATS and DGEBA. The absence of signals due to residual unreacted ATS, despite the 1:2 epoxy/amine ratio indicating a twofold excess of amine hydrogen relative to the epoxy group, suggests that each NH_2 group reacts with one epoxy with formation of secondary amines only. Differently from the 1:2 mixture, which after 15 days does not show peaks associated to the reactive sites of ATS and DGEBA

suggesting a nearly stoichiometric ring opening reaction by the primary amine group of ATS, the spectra of the 1:1 and 2:1 mixtures experience the complete disappearance of the resonance at 44.83 ppm only (α carbon of ATS) while the signals of the epoxy fragments are still well detectable. It is worth to mention that the literature reports on a conversion of 44% and 85% of the secondary aminesilane *N*-phenylaminepropyltrimethoxysilane and bis(trimethoxysililamine) when reacted with DGEBA ($M_n = 370$) at molar ratios of 1:2 and 1:3, respectively, at 90 °C [5]. Independently from the molar ratio the signals of the $Si(OC_2H_5)_3$ groups at 58.21 ppm gradually disappear being replaced by new superimposed absorptions in the same range attributable to partially hydrolyzed $Si(OC_2H_5)_{3-x}(OH)_x$ ($x = 1, 2, 3$) species [10]. The resonance at 7.39 ppm, due to the methylene carbon of the ethoxy group and the signals of the CH_2 groups in α position to the silicon atom follow the same fate being replaced by four signals falling in the same range. The combined NMR findings suggest that oxirane ring opening and hydrolysis of the alkoxy groups are concomitant processes occurring at slow rate and that the ring opening reaction is dependent on ATS concentration. The glassy solids obtained by curing the three mixtures at 25 °C for three months were investigated by FT-Raman and NIR spectroscopy. IR spectroscopy is not helpful since the epoxy breathing bands as well as absorptions of the silanole groups were not clearly detected owing to a very broad band, involving the Si–O–Si network formation, ranging from 950 to 1250 cm^{-1}. Micro-Raman spectra, used to gain microstructural informations, were not of much help in the absorption domains lying in the range 400–500 and 600–700 cm^{-1}, diagnostic of the presence of the Si–O–Si network formation and partially hydrolyzed $Si(OC_2H_5)_{3-x}(OH)_x$ ($x = 1, 2, 3$) [11] species since the parent epoxy resin shows several absorptions in this range. Nevertheless the strong polarized band due to the symmetrical $\nu(SiO_3)$ stretching of unhydrolyzed $Si(OC_2H_5)_3$ (651 cm^{-1}) [11] group of ATS was not detected. As it concerns the organic fragment, the inplane expansion and contraction of all three ring bonds, which in the starting compound is visible as a strong polarized band at 1245 cm^{-1}, appears as a shoulder in the spectra of **1**, **2** and **3** indicating that epoxy groups are not fully turned over. The content of unreacted oxirane rings, after three months of curing at room temperature, was estimated by Raman spectroscopy. Determination of the bands areas and position was carried out by curve-fitting of the experimental profile. Normalization was achieved by using, as internal standard, the band at 1612 cm^{-1} whose scattered intensity does not change as a function of the time. The data plotted in Figs. 2–4 clearly show that the conversion of oxirane rings decreases by increasing the epoxy/amine ratio, with conversion percentages ranging from 95.3 to 81.3%. These findings are also supported by absorbance NIR spectra in the 4400–5000 cm^{-1} range. The characteristic peak at 4535 cm^{-1} of pure DGEBA, due to the epoxy-ring overtone bands [12,13], is no more visible in

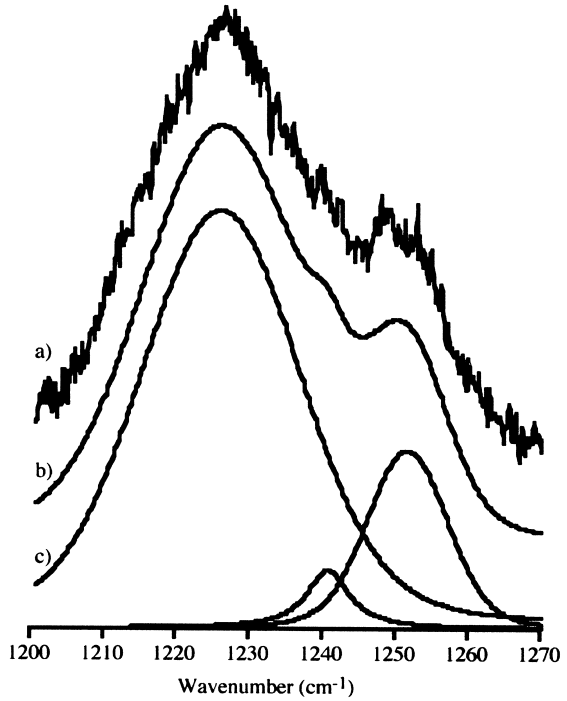

Fig. 2. Raman spectrum of sample **1** (a); global (b) and single peak (c) fitting curves obtained with PeakFit.

the spectra of **1** and **2** while it appears hardly detectable in the spectrum of **3** (Fig. 5).

The morphology and fracture surfaces of the samples **1**, **2** and **3** were studied using scanning electron microscopy. Preliminary observations on such materials proved to be unsuccessful as specimens under the electron beam rapidly

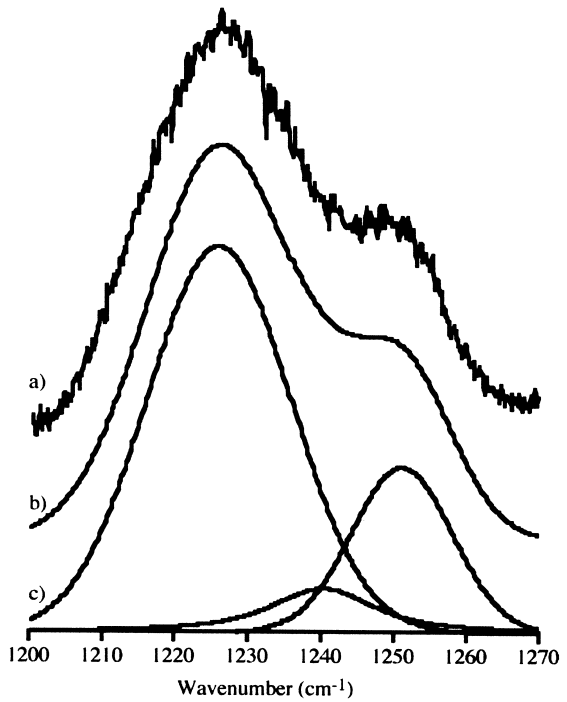

Fig. 3. Raman spectrum of sample **2** (a); global (b) and single peak (c) fitting curves obtained with PeakFit.

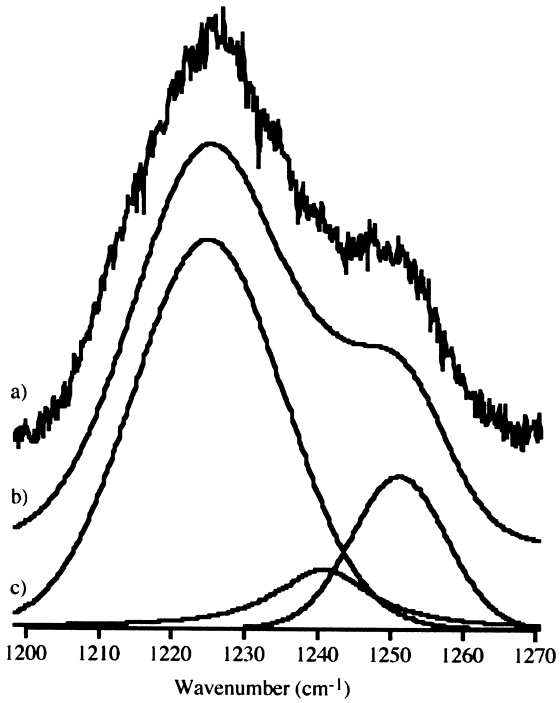

Fig. 4. Raman spectrum of sample **3** (a); global (b) and single peak (c) fitting curves obtained with PeakFit.

dissolve, showing almost instant 'burning' effects that stopped observations. This failure, ascribed to incomplete curing, was particularly evident for sample **1**. Further curing at 80 °C for four days led to specimens suitable for SEM investigations. SEM images show that all the three mixtures are featured by a uniform structure over the entire area as well as improved glassy quality with increasing the ratio DGEBA/ATS. Surface observations show substantially a great homogeneity with absence of cracks, veins and/or fissures and without formations of clusters and/or aggregates. No pores or significant surfaces modifications, due to the different molar ratios, were observed up to 40000 X. While the SEM images of **1** an **2** show featureless flat surfaces (figures omitted because not significant), sparse voids and small (200 nm in length) elongated structures, located 'in relief' on the polymer surface, were detected on the entire surface of sample **3** (Fig. 6). The 'relief' of these structures, featured by a preferential oriented elongation, is only about 10 nm.

The thermal properties of mixtures **1**, **2** and **3** were investigated by TGA in dynamic nitrogen and air atmosphere. As a common feature, the presence in **1**, **2** and **3** of Si–O–Si linkages increases the polymer degradation temperature and thermal oxidative stability relative to the parent epoxy resin by shifting the weight loss to higher temperatures. Fig. 7, which reports the TGA curves of the different DGEBA/ATS mixtures under nitrogen flow, features the positive effect of the ATS component on the thermal stability of the polymers which increases in the order **1** > **2** > **3**. By way of comparison the thermogravimetric curve of DGEBA, showing the rapid thermodegradation of the starting polymer that is heat-stable up to 220 °C, is also reported. Furthermore the observation of the derivative traces (Fig. 8) makes easier to detect the increase of the PDT (Polymer Degradation Temperature) with the decreasing of the DGEBA/ATS ratio. The thermal degradation of **1**, **2** and **3** in dynamic nitrogen occurs in two well defined steps: a) a low temperature weight loss mainly due to the removal of residual condensation products, alcohols or water, pre-formed during the 'ageing' of the mixture or produced during the 'cooking' following the thermogravimetric scanning; b) the main decomposition process, related to the thermal stability of the investigated mixtures, which occurs in two steps. The quantitative characterization of degradation process, temperatures of maximum volatilization rate and residues for each step are well shown in Table 1. The weight loss curves clearly show that the rate of degradation of crude DGEBA is largely reduced following ATS incorporation and that **2** shows the fastest thermal degradation kinetic, despite its relative weight loss (36.1%) is superior with respect to the values found for **1** (20.7%) and **3** (23.7%). Furthermore the onset of polymer decomposition improves as a greater amount of ATS component is

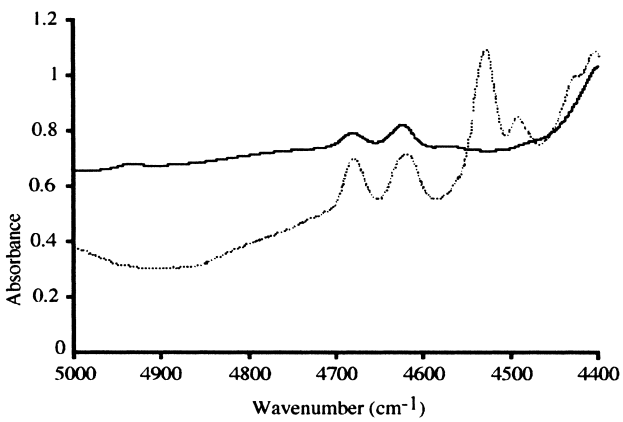

Fig. 5. NIR spectrum of sample **3** (solid line) and of pure DGEBA (dashed line).

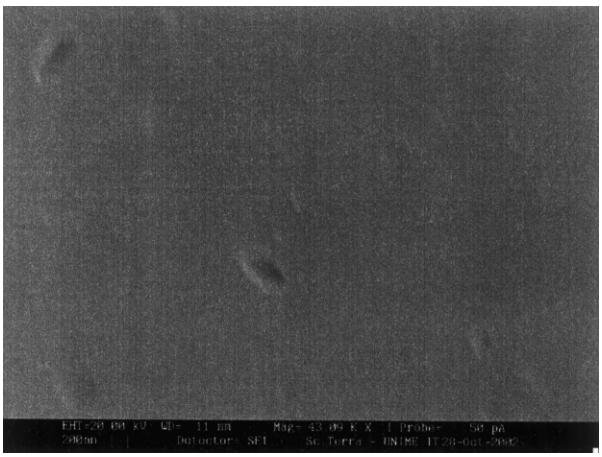

Fig. 6. SEM image for sample **3**. Magnification 43000 X.

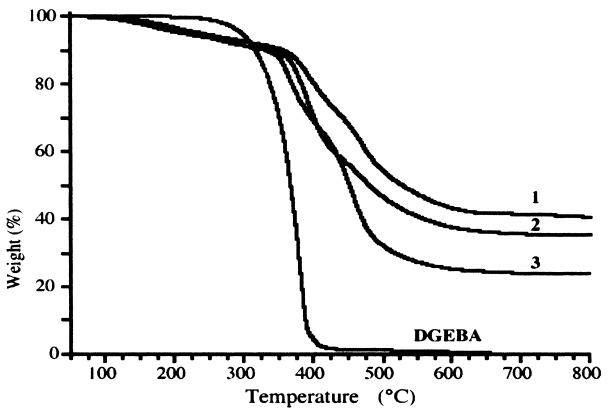

Fig. 7. TGA curves of samples **1**, **2**, **3** and pure DGEBA showing the effect of the abundance of ATS on thermal stability (under Nitrogen flow).

inversion of abundance. **2** shows the slowest thermal degradation process and the smallest weight loss (29.1% against 30.8 and 43.3% for **1** and **3**, respectively). The abundance of the obtained residue is, respectively, **1** > **2** > **3** and qualitatively mirrors the abundance of the initial ATS content.

From the DSC analysis (traces not reported), a quite broad endothermic process that starts at ~50 °C and ends at ~280 °C emerges for each sample; the width of the process and its slow evolution suggests an 'entrapment' phenomenon with a slow release of volatiles after being trapped in the pore network as secondary products of the polymerization. At temperatures higher than 280 °C, the thermal processes observed are due to the thermal degradation of the composite. No residual enthalpy

Table 1
Thermogravimetric results obtained for DGEBA and DGEBA/ATS mixtures in temperature range of 50–800 °C, under N_2 flow (50 mL/min)

	DGEBA	DGEBA/ATS **1**	DGEBA/ATS **2**	DGEBA/ATS **3**
First event				
T_{init} (°C)	–	85	85	85
Tv_{max} (°C)	–	166	193	181
T_{final} (°C)	–	288	282	306
Δm (%)	–	7.3	6.5	9.0
Second event				
T_{init} (°C)	215	288	282	306
Tv_{max} (°C)	384	394	394	365
T_{final} (°C)	472	432	445	407
Δm (%)	98.6	20.7	36.1	23.7
Third event				
T_{init} (°C)	–	432	445	407
Tv_{max} (°C)	–	473	474	454
T_{final} (°C)	–	681	684	682
Δm (%)	–	30.8	21.9	43.3
Residual mass				
Res. 800 °C (%)	0	40.5	35.0	23.5

incorporated into the epoxy network. The higher temperature thermogravimetric step shows that the degradation behavior is similar for the three mixtures but the degradation rate as well as the percentage of lost material indicate an

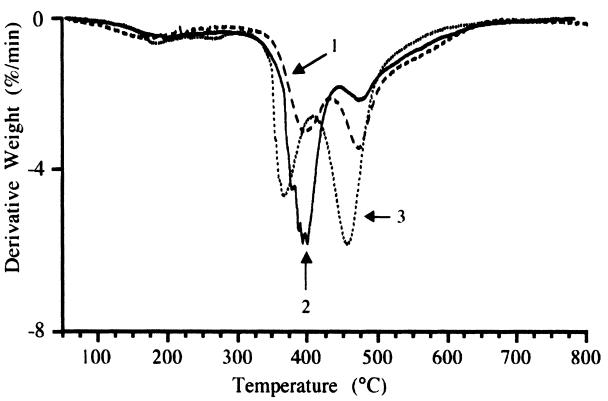

Fig. 8. Derivative thermogravimetric curves of samples **1**, **2**, **3** and pure DGEBA (under Nitrogen flow).

curing peaks were observed. Glass transition temperature measurements show that, differently from **2** and **3** which show a glass transition at 90 °C, **1** does not exhibit any detectable glass transition. These results, based on DSC measurements only, suggest that systems richer in ATS is featured by a high degree of cross-linking which, beside to increasing the thermal stability of the network, decreases the segmental mobility of the polymer with the consequent disappearance of the glass transition.

To verify the thermal stability of the mixtures DGEBA/ATS and their residues in an oxidative environment, the thermogravimetric experiments have also been carried out in air. In Table 2 are summarized degradation temperatures and weight loss values for the mixtures heated in air atmosphere (50 mL/min). Fig. 9 shows that the presence of the inorganic phase increases the thermo-oxidative stability relative to uncured DGEBA by shifting the weight loss curve to higher temperatures. Furthermore the presence of oxygen during heating does not entail specific differences in

Table 2
Thermogravimetric results obtained for DGEBA/ATS mixtures in temperature range of 50–800 °C, under Air flow (50 mL/min)

	DGEBA/ATS **1**	DGEBA/ATS **2**	DGEBA/ATS **3**
First event			
T_{init} (°C)	80	80	80
Tv_{max} (°C)	170	166	175
T_{final} (°C)	254	273	287
Δm (%)	6.6	6.2	9.0
Second event			
T_{init} (°C)	254	273	287
Tv_{max} (°C)	388	398	356
T_{final} (°C)	447	436	399
Δm (%)	15.8	19.8	20.0
Third event			
T_{init} (°C)	447	436	399
Tv_{max} (°C)	454	453	436
T_{final} (°C)	533	534	547
Δm (%)	27.6	27.0	40.7
Fourth event			
T_{init} (°C)	533	534	547
Tv_{max} (°C)	623	640	626
T_{final} (°C)	706	745	710
Δm (%)	30.0	30.72	22.2
Residual mass			
Res. 800 °C (%)	20.0	16.28	8.16

the degradation pattern of **1**, **2** and **3** except a further decomposition step at temperature higher than 500–600 °C. Very likely the fourth degradation step arises from the combustion of the polymeric residue not previously oxidized. From the comparison of data obtained in N_2 flow and those collected in air, it can be noticed that an additional degradation step occurs associated with an increasing in some weight losses. This phenomenon is in keeping with the oxidation and/or sublimation of the degradation products of the analyzed samples. Furthermore, this phenomenon becomes less fast on going from the lower ones to the higher DGEBA/ATS ratios mixtures, whereas a corresponding increase of weight loss is also registered. The final residue is composed of inorganic and carbonaceous substances.

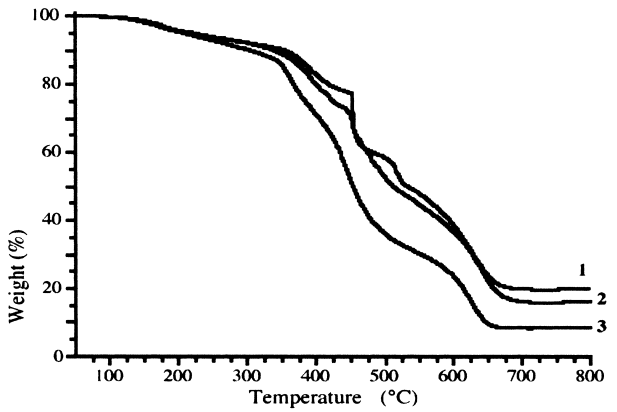

Fig. 9. TGA curves of samples **1**, **2** and **3** showing the effect of the abundance of ATS on the thermal stability (under Air flow).

The different thermogravimetric behaviour of **1**, **2** and **3** may be explained in terms of the different polymeric networks arising from different growing and/or cross-linking processes of the pre-polymers. In mixture **1** and **2** ATS acts as a co-reactant and represents an integral part of the final polymeric network. So the mechanical and thermal properties of **1** and **2** are more influenced by the chemical nature of ATS. This influence decreases on going from **1** to **3** whose properties are more imparted by the chemical structure of DGEBA while ATS mainly acts as a catalyst. Furthermore the growing number of Si–O–Si linkages on going from **3** to **1** produces a more intimate structure with consequent repercussion on their mechanical and thermal properties.

4. Conclusions

Room temperature reaction of the epoxy resin poly(bisphenolA-*co*-epichlorohydrin), glycidyl end-capped with ATS leads to the formation of homogeneous, insoluble inorganic modified epoxy polymers. ^{13}C NMR, NIR and Raman spectroscopy findings show that a very high percentage of cleaved epoxy rings corresponds to the lower ratio DGEBA/ATS mixture. The growing presence of siloxane linkages within the polymer backbone of **1**, **2** and **3**, which are featured by little discernible differences in morphology, increases the onset of the thermal degradation while the different molar ratio leads to different polymeric networks. The inorganic phase in **1**, being predominant, acts as a network former while in **3** it mainly acts as a network modifier. Furthermore the motion of the organic polymer is restricted as a function of the Si–O–Si linkages with consequent repercussions on mechanical and thermal properties. Conservative experiments on selected lithotypes, appropriately treated with **1**, **2** and **3**, are at the moment in due course aimed to test their efficacy as conserving materials.

Acknowledgements

This work was supported by the Ministero dell'Università e della Ricerca Scientifica (Murst) of Italy.

References

[1] Selwitz CM. Mater Res Soc Symp Proc 1992;267:925–34.
[2] Ginell WS, Kotlik P, Selwitz CM, Wheeler GS. Mater Res Soc Symp Proc 1995;352:823–9.
[3] Cardiano P, Sergi S, Lazzari M, Piraino P. Polymer 2002;43:6635–40.
[4] Ochi M, Takahashi R, Terauchi A. Polymer 2001;42:5151–8. and references therein.

[5] Mascia L, Tang T. J Mater Chem 1998;8:2417–21.
[6] Landry MR, Coltrain BK, Landry CJT, O'Reilly JM. J Polym Sci, Polym Phys Ed 1995;33:637–55.
[7] Nishijima S, Hussain M, Nakahira A, Okada T, Niihara K. Mater Res Soc Symp Proc 1996;435:243–8.
[8] Hussain M, Nishijima S, Nakahira A, Okada T, Niihara K. Mater Res Soc Symp Proc 1996;435:369–74.
[9] Riegel B, Blittersdorf S, Kiefer W, Hofacker S, Muller M. J Non-Cryst Solids 1998;226:76–84.
[10] Templin M, Wiesner U, Spiess HW. Adv Mater 1997;9:814–7.
[11] Artaky I, Bradley M, Zerda TW, Jonas J. J Phys Chem 1985;89: 4399–404.
[12] Poisson N, Lachenal G, Sautereau H. Vib Spectrosc 1996;12:237–47.
[13] Lyon RE, Chike KE, Angel SM. J Appl Polym Sci 1994;53:1805–12.